JOURNAL OF ADVANCED DIELECTRICS
Vol. 10, No. 4 (2020) 2050011 (9 pages)

DOI: 10.1142/S2010135X20500113

Effect of sintering temperature on the dielectric, ferroelectric and energy storage properties of SnO_2-doped $Bi_{0.5}(Na_{0.8}K_{0.2})_{0.5}TiO_3$ lead-free ceramics

Nguyen Truong-Tho*,‡ and Le Dai Vuong†
*Department of Physics, College of Sciences
Hue University, Hue City, Vietnam
†Faculty of Natural Sciences
Thu Dau Mot University
Binh Duong Province, Vietnam
‡truongtho@hueuni.edu.vn

Received 3 February 2020; Revised 28 April 2020; Accepted 8 June 2020; Published 22 July 2020

Sintered lead-free $Bi_{0.5}(Na_{0.8}K_{0.2})_{0.5}(Ti_{0.96}Sn_{0.04})O_3$ ceramics (BNKTS) have been fabricated via a solid-state reaction. The effect of sintering temperature on the structural, morphological, dielectric, ferroelectric and energy storage properties of BNKTS ceramics was investigated, and it was found that the electrical properties of the synthesized ceramics increased with the increase in the sintering temperature, and the highest values were achieved at 1100°C. The ceramics sintered at the optimized temperature of 1100°C exhibited the best physical, dielectric, ferroelectric and energy storage properties, namely, high density (the relative density, $\rho = 5.88\,g.cm^{-3}$, approximate to 96.7% of the theoretical value), high densification factor (DF = 0.93), high dielectric constant ($\varepsilon_r = 1215$), low dielectric loss ($\tan\delta = 0.051$), highest dielectric constant ($\varepsilon_{max} = 4335$), high remanent polarization ($P_r = 9.5\,\mu C.cm^{-2}$), high coercive field ($E_c = 14.3\,kV/cm$), high energy storage density ($0.12\,J/cm^3$), and high energy storage efficiency (41.7% at 46.3 kV/cm).

Keywords: Lead-free ceramics; BNKT; sintering temperature; dielectric constant.

1. Introduction

In recent years, lead-free piezoelectric ceramics have attracted great attention, leading to the discovery of many new ceramics with excellent physical properties as well as widespread applications.[1–7] There have been many approaches to synthesize lead-free piezoelectric ceramics.[8,9] Among several lead-free ceramics, $Bi_{0.5}Na_{0.5}TiO_3-Bi_{0.5}K_{0.5}TiO_3$-based systems with the concentrations corresponding to the existence of rhombohedral–tetragonal mixed phases known as morphotropic phase boundary (MPB) have considerable interest in research in the recent year to improve piezoelectric properties.[10–12] Thus, some peroveskite ceramics based on $Bi_{0.5}(Na_{0.8}K_{0.2})_{0.5}TiO_3$ (BNKT) were fabricated and characterized in this study. Moreover, the serious problem during sintering bismuth-related materials is the easy evaporation of bismuth ions at high temperature.[13–16] Therefore, dielectric breakdown occurs easily at a low electric field. To overcome this problem, in our preliminary work on fabricating BNKT ceramics by solid state reaction, BNKT ceramics were doped with some various sintering aids such as Zn^{2+} and Li^+ ions.[17,18] For examples, by adding ZnO in nano grain size into BNKT ceramics, we not only decreased sintering temperature but also improved piezoelectric property of as-synthesized products. The formation of the Bi_2O_3-ZnO liquid phase at 738°C of eutectic temperature during annealing process makes sintering temperature decrease.

Similarly, the ion radii of Sn^{4+} (0.069 nm) and Ti^{4+} (0.0605 nm) ions are approximated so that Sn^{4+} can occupy the position of Ti^{4+} in BNKT crystals. Goldschumidt's tolerance factors of the BNKT doped with Sn^{4+} are smaller than those of the pure BNKT ($t_{BNKT} = 0.868$).[18] Therefore, the lattice distortion is due to the addition of Sn^{4+} ions. This implies that the value of dipole moment will be increased so that the piezoelectric property of BNKT doped with Sn^{4+} ions was enhanced. Moreover, Mokhtari *et al.* also showed the existance of the Sn–Bi liquid phase at the eutectic temperature of 170°C.[19] Furthermore, the energy storage density enhanced significantly with the high W_{rec} of $2.35\,J/cm^3$ was achieved in 1% mol SnO_2-doped $Sr_{0.6}(Na_{0.5}Bi_{0.5})_{0.4}TiO_3$ ceramics with high energy storage efficiency (η) of 80% under an electric field of 180 kV/cm.[20,21] Therefore, the fabrication of $Bi_{0.5}(Na_{0.8}K_{0.2})_{0.5}(Ti_{1-x}Sn_x)O_3$ ceramics at low temperature would enable the way to improve the piezoelectric property of BNKT ceramics.

As Sn-doping level increased up to 5 at.% in $Bi_{0.5}(Na_{0.82}K_{0.18})_{0.5}TiO_3$, a transition to an ergodic relaxor behavior was evidenced by a strong frequency-dependent dispersion in the dielectric permittivity and the appearance of a

giant strain with a constriction in $P(E)$.[22] Moreover, all specimens of $Bi_{0.5}(Na_{0.82}K_{0.18})_{0.5}(Ti_{1-x}Sn_x)O_3$ had perovskite symmetry while a trace of SnO_2 was observed as a secondary phase when $x > 0.05$, which seemed to be the solubility limit of Sn in BNKT. When $x > 0.03$, specimens showed little piezoelectric response even after poling treatment at elevated temperatures. This suggests that the Sn-doping induced pseudocubic phase ($x > 0.03$) is nonpolar at low electric fields.[23] That is the reason the SnO_2 content of 0.04 mol is selected in this experiment, by which we have studied the effect of sintering temperatures on the structural, morphological and electrical properties of $Bi_{0.5}(Na_{0.8}K_{0.2})_{0.5}(Ti_{0.96}Sn_{0.04})O_3$ ceramics.

2. Experimental

A conventional solid-state reaction route was applied to prepare $Bi_{0.5}(Na_{0.8}K_{0.2})_{0.5}(Ti_{0.96}Sn_{0.04})O_3$ (BNKTS) ceramics. Starting raw materials, namely, Bi_2O_3 (Merck, ≥99.5%), TiO_2 (Merck, ≥99.5%), Na_2CO_3 (Merck, ≥99.5%), K_2CO_3 (Merck, ≥99.5%), and SnO_2 (Merck, ≥99.5%) were weighed, and then milled via ultrasonic treatment in ethanol for 1 h. In order to identify the temperature for calcining BNKTS ceramics, we investigated the thermogravimetric analysis (TGA) and differential thermal analysis (DTA) data of BNKTS powders, as shown in Fig. 1. Accordingly, the TGA curve of the mixture powder shows that the total mass decreased with temperature. The first region, where the temperature is below 200°C with an endothermic peak at 87°C, corresponds to the evaporation of the residual nonstructural water and solvents in the sample, and the corresponding weight loss of the sample is about 5.97%. The next region at 469.2°C indicates an exothermal effect with 6.37% weight loss. This is attributed to the decomposition of Na_2CO_3 and K_2CO_3 and their mechanical mixing with Bi_2O_3, TiO_2, and SnO_2, which consequently react to form BNKTS. The formation of BNKTS is completed at about 745°C.

According to the figure, the phase structure of the material is, in principle, formed at a temperature of 745°C. However, the initial mass of the mixture in the stoichiometric proportion used for measuring TGA-DTA curves is very small compared with the amount of the raw materials used in the actual preparation in our experiments. It is the main reason the calcining temperatures in most of the studies fabricating BNKT ceramics by solid-state reaction were 850°C.[17,18,22,23] Similarly, 850°C was selected as the calcining temperature for 2 h to synthesize the BNKTS compounds. The calcined BNKTS compounds were then milled for 20 h. Next, the ground materials were pressed into disks of 12 mm diameter and 1.5 mm thickness under 100 MPa. The samples were sintered at 1000°C, 1050°C, 1100°C, 1150°C and 1200°C for 2 h.

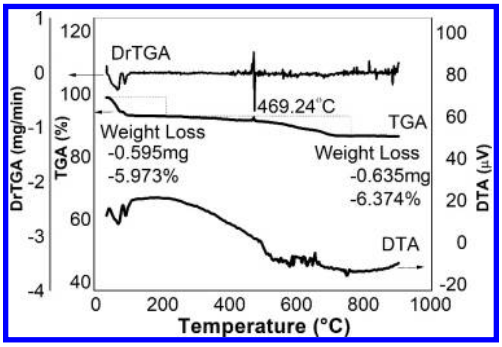

Fig. 1. TGA and DTA curves of BNKTS power at 10°C/min heating rate.

The properties of the samples were studied by different analytical methods. The X-ray diffraction (XRD) analysis (Rigaku RINT 2000) was carried out at room temperature to explore the crystallinity of the samples. Field-emission scanning electron microscopy (Nova NanoSEM 450-FEI-HUS-VNU) was employed to examine the morphologies of the as-prepared ceramics. The structural analysis was carried out by the Rietveld refinement method in the FullProf program. Furthermore, the density and ferroelectric loops of the samples were measured by the Archimedes principle and the Sawyer–Tower method, respectively. Moreover, the grain size was determined by the mean linear intercept method. Finally, the dielectric properties of the samples were measured by analyzing the temperature dependencies of capacitance and phase angle (HIOKI 3532).

3. Results and Discussion

Table 1 shows the variations in the density of $Bi_{0.5}(Na_{0.8}K_{0.2})_{0.5}(Ti_{0.96}Sn_{0.04})O_3$ ceramic samples at different sintering temperatures. When the sintering temperature was increased from 1000°C to 1200°C, the density of the samples increased from 4.89 to 5.88 g/cm^3, reaching the highest value of 5.88 g/cm^3 (relative density: 96.7% of the theoretical value) at 1100°C, beyond which it subsequently decreased. The variation in the densification behavior of the ceramics during sintering can be explained by the defect chemistry and the creation of oxygen vacancies.[24,25] It is well known that Na^+, K^+, and Bi^{3+} volatilize during the sintering process. The volatilization of these ions produces

Table 1. Density, relative density, densification, and total shrinkage after sintering of BNKTS ceramics as a function of sintering temperatures.

Sintered temperatures (°C)	Density (g/cm^3)	Relative density (%)	Densification factor	Shrinkage after sintering (%)
1000	4.89	80.4	0.56	10.83
1050	5.34	87.8	0.72	13.33
1100	5.88	96.7	0.93	14.67
1150	5.78	95.1	0.89	14.83
1200	5.71	93.9	0.86	14.75

oxygen vacancies in the ceramics according to the Kröger–Vink equation as follows[26]:

$$2K_K^x + O_O^x \rightarrow 2K_K' + V_O^{oo} + K_2O, \quad (1)$$

$$2Na_{Na}^x + O_O^x \rightarrow 2Na_{Na}' + V_O^{oo} + Na_2O, \quad (2)$$

$$2Bi_{Bi}^x + O_O^x \rightarrow 2Bi_{Bi}''' + 3V_O^{oo} + Bi_2O_3. \quad (3)$$

In other words, the presence of oxygen vacancies in materials is advantageous for mass transport during sintering in ceramics. Hussain *et al.* reported that the number of vacancies generally increases with an increase in the sintering temperature.[25] At lower temperatures, a number of oxygen vacancies are small and the ability of the atoms to diffuse is also small. Hence, the lower density of the $Bi_{0.5}(Na_{0.8}K_{0.2})_{0.5}(Ti_{0.96}Sn_{0.04})O_3$ ceramics sintered at 1000°C and 1050°C is due to poor diffusion and insufficient sintering of the ceramics. However, the poor densities found at 1150°C and 1200°C may be due to the evaporation of the volatile alkali metal oxide, according to Eqs. (1)–(3).

As shown in Table 1, the densification factor (DF) of ceramics at different temperatures can be obtained by using Eq. (4):

$$DF = \frac{\rho_m - \rho_g}{\rho_t - \rho_g}, \quad (4)$$

where ρ_t is the theoretical density, ρ_m is the measured density, and ρ_g is the density of green pellets without sintering.[27] The densification factor increased with the increase in temperature until it reached the highest value of 0.93 at 1100°C, and then decreased. Due to the densification mechanisms and thermal contraction, a positive densification factor indicates shrinkage of ceramics at sintering temperatures.[28] A positive DF indicates shrinkage. Table 1 also expresses the shrinkage ratio of the ceramics as a function of sintering temperature. While the shrinkage ratio exhibits an increasing trend from 10.83% to 14.83% up to the sintering temperature of 1150°C, it decreased slightly above that temperature. The relation between the sintering temperature and shrinkage ratio depends on thermal dilatation.[28]

Figure 2(a) shows the XRD patterns of the $Bi_{0.5}(Na_{0.8}K_{0.2})_{0.5}(Ti_{0.96}Sn_{0.04})O_3$ ceramics sintered at different temperatures from 1000°C to 1200°C in the 2θ range from 20° to 70°. The study revealed a pure perovskite phase of the BNKTS ceramics up to the sintering temperature of 1150°C. However, a secondary phase appeared at the sintering temperature of 1200°C, as denoted by the triangle in the XRD pattern, and it was identified as the pyrochlore phase. The formation of the pyrochlore phase in ceramics may be due to either the incomplete conversion of the intermediate pyrochlore structure into perovskite structure or the evaporation of Bi and alkali metal (Na, K) at high temperatures during the sintering process, which may have caused the formation of nonstoichiometric structural defects in the $Bi_2Ti_2O_7$ pyrochlore phase, as reported in the ICPDS File No. 32–0118.[29,30] According to Kargin *et al.*, bismuth titanate exists in equilibrium with the pyrochlore structure within the temperature range of 1000°C–1210°C. This phase is not strictly stoichiometric because the synthesis at high temperatures leads to the formation of cation-deficient samples.[31] Therefore, excessive Bi_2O_3, Na_2CO_3, and K_2CO_3 were taken into account for volatility during the calcination process while maintaining the stoichiometry of the synthesized BNKTS ceramics. The results indicated that the sintering temperature was an important parameter in obtaining a stable phase structure.[32] Furthermore, the inset in Fig. 2(a) illustrates the detailed XRD analysis in the 2θ range of 42–47°. $Bi_{0.5}Na_{0.5}TiO_3$ is rhombohedral, whereas $Bi_{0.5}K_{0.5}TiO_3$ is tetragonal at room temperature[24] The splitting of $(002)_T$ and $(200)_T$ peaks indicates the ferroelectric tetragonal phase (T), while the single $(200)_R$ peak implies the ferroelectric rhombohedral phase (R). Moreover, triplet peaks indicate that the samples consist of the mixture of tetragonal and rhombohedral phases.[33] When the sintering temperature increased from 1000°C to 1200°C, the rhombohedral relative fraction decreased, while the tetragonal relative fraction increased, as demonstrated in Fig. 2(b). This was evidenced by the stronger peak splitting of $(002)_T$ and $(200)_T$, implying an increase in the tetragonality (c/a) values with increase of sintering temperature. This result is consistent with the analysis result the Rietveld refinement technique, as shown in Fig. 3.

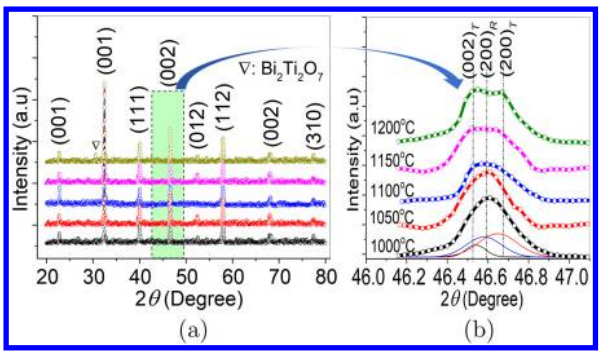

Fig. 2. The XRD patterns of $Bi_{0.5}(Na_{0.8}K_{0.2})_{0.5}(Ti_{0.96}Sn_{0.04})O_3$ ceramics with 2θ ranging from (a) 20° to 80°, and (b) 46–47°.

The presence of both rhombohedral (*R3c*, the samples were sintered at 1100°C) and tetragonal (*P4bm*, the samples were sintered at 1200°C) crystal symmetries was confirmed by the Rietveld refinement technique (Figs. 3(a) and 3(b)). The fitting analysis of peak shape and peak position, structure and background was performed in terms of profile *R*-factors (Table 2). The coexistence of two different structural phases was detected in the samples, and the MPB with the rhombohedra phase fraction (*R3c*) above 60% was formed at sintering temperature of 1150°C and 1200°C. On further refinement (sintering temperature is less than 1100°C), the rhombohedral symmetry was found to fit well ($M_R = 100\%$, Table 2).

In order to clarify the effect of sintering temperatures on the microstructure of the BNKTS ceramics, we sintered the samples from 950°C to 1200°C for 2 h. As shown in Fig. 4,

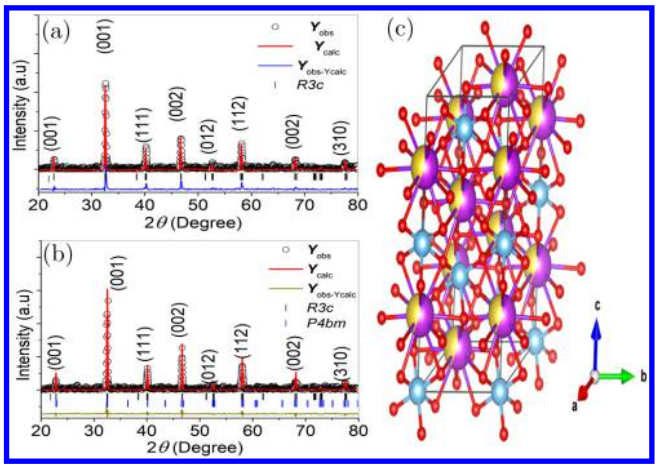

Fig. 3. (a,b) Rietveld refined XRD patterns of $Bi_{0.5}(Na_{0.8}K_{0.2})_{0.5}(Ti_{1-x}Sn_x)O_3$ ceramics, and (c) View of the BNKTS lattice cells is visualized in rhombohedral cell with a space group of *R3c*.

the shape of grains in all samples is rectangular with the dense microstructure and clear grain boundary. The grain size increases with the increase of sintering temperatures and reaches the maximum value of 1.18 μm at 1200°C in Fig. 4. In this study, the grain sizes are located between 0.27 and 1.18 μm and gathered around the top of the Gauss fitting plot in Fig. 5. The low melting point of the Bi–Sn system is beneficial to generate a eutectic liquid phase at 170°C.[19] This is considered to be rational; thus, this phase can work as a lubricant during the sintering process, wetting solid particles and providing capillary pressure between them, resulting in faster grain growth of the ceramics.[34,35] However, when the sintering temperature was raised to 1200°C, the grain profile of the ceramic changed to rough with small porosity, which may be the reason for the deterioration of its density as shown in Table 1.

The effect of sintering temperatures on the dielectric constant (ε_r) and dielectric loss (tanδ) of the BNKTS ceramics at 1 kHz is illustrated in Fig. 6. When sintering temperatures of the ceramics were increased from 1000°C to 1200°C, the values of ε_r increased proportionally and reached the maximum of 1215 at the sintering temperature of 1100°C, and then decreased. On the other hand, values of tanδ decreased on increasing the sintering temperature. The minimum, tan$\delta = 0.051$, was obtained at the sintering temperature of 1100°C, which increased further on increasing the sintering temperature. The high dielectric constant at the sintering temperature of 1100°C can be attributed to the high density, larger grain size and improved crystalline quality.[24]

Figure 7 shows the temperature dependence of ε and tanδ for the $Bi_{0.5}(Na_{0.8}K_{0.2})_{0.5}(Ti_{0.96}Sn_{0.04})O_3$ ceramics at 1 kHz. They underwent two phase transitions in the measured temperature range included as T_m (dielectric constant peak, $T_m \approx 260$°C) and T_{F-R} (frequency dispersion, $T_{F-R} \approx 115$°C). Some studies found strong frequency-dispersed presents around T_{F-R}, whereas it is less notable and negligible frequency dispersion at T_m. These broad peaks do not involve any structural transformation and an intermediate weakly polar phase exists between T_{F-R} and T_m named as ergodic relaxor (ER) phase. The origin of anomalies is associated with the polar nanoregions (PNRs).[36–38] Maqbool *et al.* suggested that the temperature of T_{F-R} is the ferroelectric-to-relaxor transition point due to thermal evolutions of discrete PNRs.[39] The lower dielectric peaks at T_{F-R} exhibited strong frequency dependence, implying that the ceramics underwent relaxation or phase transition at T_{F-R}.[40]

Moreover, the formation of vacancies causes a significant change in the lower phase transition at T_{F-R} in Fig. 8. Some researchers have suggested that the shift of T_{F-R} for many lead-free ceramics can be related to Bi, K, and/or Na loss during the processing.[41,42] Yoshii *et al.* said that the possible twisting of the oxygen octahedron near the MPB, the T_{F-R} of BNKT ceramics will decrease sharply near the MPB.[43] When sintering temperatures of ceramics increase from 1000°C to 1200°C, the values of ε_{max} increase proportionally and reach to the maximum of 4335 corresponding to $T_m = 262$°C at the sintering temperature of 1100°C, and then ε_{max} decrease as shown in Fig. 8. This implies that the lattice distortion was affected by the sintering temperature as discussed above on the XRD patterns in Table 2, which resulted in the change of T_m and ε_{max}. As can be seen in Fig. 8, the maximum dielectric constant ε_{max} increased with increasing the sintering temperature, and, the highest dielectric constant at 1100°C, and then sharply decreased beyond this point. It is reasonable when the surface morphology of the BNKTS ceramic

Table 2. Crystal structure parameters of BNKTS ceramics calculated by the Rietveld refinement of XRD patterns.

	R3c				*P4bm*			
The sintering temperatures	$a = b$ (Å)	c (Å)	R_{Brag}	M_R (%)	$a = b$ (Å)	c (Å)	R_{Brag}	M_T
1000°C	5.5047	13.5341	8.4	100	—	—	—	—
1050°C	5.5047	13.5341	8.4	100	—	—	—	—
1100°C	5.5047	13.5341	11.7	100	—	—	—	—
1150°C	5.496	13.5063	10.7	73.5	5.5154	3.8999	7.9	26.5
1200°C	5.4914	13.5320	9.8	61	5.5154	3.8999	9.8	39

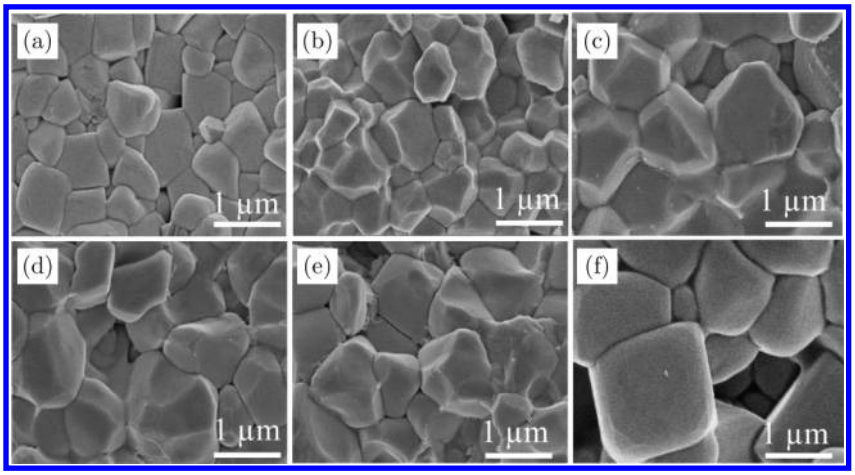

Fig. 4. Typical SEM images of the BNKTS ceramics with various sintering temperatures of (a) 950°C, (b) 1000°C, (c) 1050°C, (d) 1100°C, (e) 1150°C and (f) 1200°C.

annealed at 1100°C shows the large and homogeneous grain size with the minimum amount of mismatched hollows in Fig. 4.

In order to further confirm the effects of sintering temperature on the diffuse phase transition of $Bi_{0.5}(Na_{0.8}K_{0.2})_{0.5}(Ti_{0.96}Sn_{0.04})O_3$ ceramics, the diffuseness (γ) was evaluated by plotting $\ln(1/\varepsilon - 1/\varepsilon_{max})$ versus $\ln(T - T_m)$ (Eq. (5) at 1 kHz and temperatures greater than T_m in Fig. 9.[18] When sintering temperatures varied from 1000°C to 1200°C, the values of γ changed from 1.46 to 1.68. The variation in the γ values of the ceramics with sintering temperatures can be explained by the defect chemistry and the creation of oxygen vacancies.[24] Such vacancies made the B-site ion location shift off the center, which increased the electric dipole moment in each cell and enforced the spontaneous ferroelectric-to-relaxor phase transition.[44]

The hysteresis loops of polarization versus electric field of the $Bi_{0.5}(Na_{0.8}K_{0.2})_{0.5}(Ti_{0.96}Sn_{0.04})O_3$ ceramics sintered at 1000°C, 1050°C, 1100°C, 1150°C and 1200°C measured at room temperature are depicted in Figs. 10(a)–10(e). With the increase in the sintering temperature from 1000°C to 1200°C, the remanent polarization (P_r) increases, reaches the highest value (9.5 μC/cm^2) at 1100°C, and then decreases, while the coercive field E_C fluctuates with the increase in the sintering temperature and reaches the lowest value (14.3), as shown in Fig. 11(a). This finding is in good agreement with the study of dielectric properties and the density of the samples at different temperatures. Furthermore, polarization

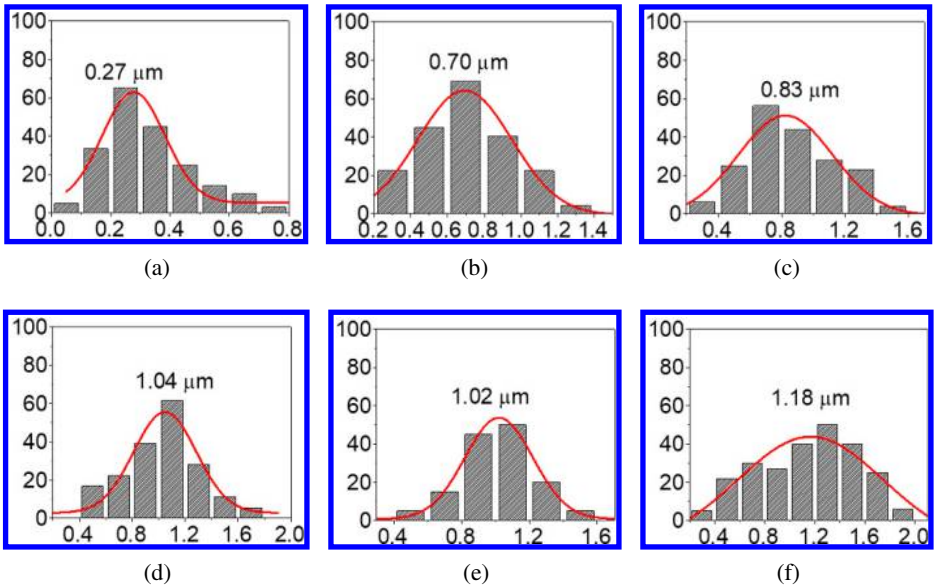

Fig. 5. Grain size distribution for the BNKTS ceramics at different sintering temperature: (a) 950°C, (b) 1000°C, (c) 1050°C, (d) 1100°C, (e) 1150°C and (f) 1200°C.

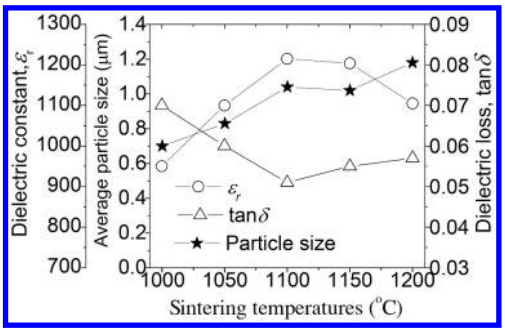

Fig. 6. Average grain size, the dielectric constant, and dielectric loss for the BNKTS ceramics as a function of sintering temperatures.

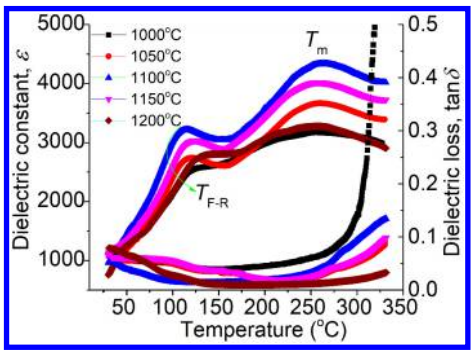

Fig. 7. Representative plot (BNKT ceramics) of relative ε and tanδ versus temperature.

increases with the increase in the density of the ceramics.[45] In other words, the larger grains, dense microstructure, and fewer grain boundaries will make the ferroelastic domain wall-reversal easier.[46] As previously discussed, the grain size and density increased with the increase in sintering temperature, which helped improve the polarization of the ferroelectric ceramics. At 1100°C, the sample has the highest density, corresponding to the highest polarization.

However, on further increasing the sintering temperature (1200°C), although the particle size increases, the ferroelectric properties of the ceramics decrease. This can also be attributed to the high ease of evaporation of volatile alkali metal oxides (Na^+, Bi and K^+) during the sintering process

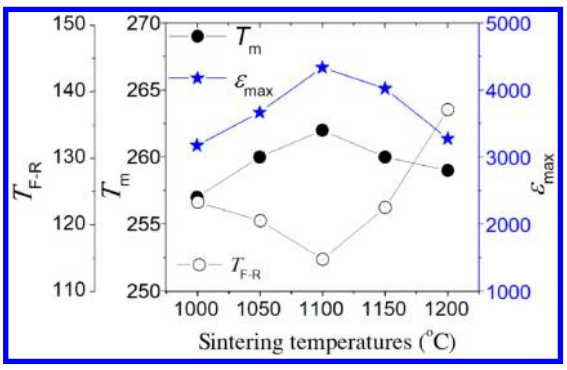

Fig. 8. The dependence of the values of ε_{max}, T_m, and T_{F-R} versus sintering temperature.

when the sintering temperature of the sample is too high.[47] Cao *et al.* derived an empirical equation to measure not only the deviation in the polarization axis but also that in the electric field axis, as follows:

$$R_{sq} = \frac{P_r}{P_s} + \frac{P_{1.1E_C}}{P_r}, \tag{5}$$

where R_{sq} is the squareness of the hysteresis loop, P_r is the remnant polarization, P_s is the saturation polarization, and $P_{1:1Ec}$ is the polarization at an electric field equal to 1.1-fold of the coercive field.[48] When the sintering temperature was varied from 1000°C to 1200°C, the values of R_{sq} changed to 0.65, 0.67, 0.64, 0.50, and 0.49. This behavior is similar to those stated in the previous report for BNKT-based ceramics.[6]

The energy storage density W_1 (Fig. 10(f), marked in green area) was obtained by integrating the area between the polarization axis and the discharge curve of the unipolar $P-E$ hysteresis loops using Eq. (6):

$$W_1 = \int_{P_r}^{P_{max}} E\mathrm{d}P. \tag{6}$$

The energy storage efficiency (η) of the material can be calculated by Eq. (7)[49]:

$$\eta = \frac{W_1}{W_1 + W_2}. \tag{7}$$

The varying trend in the energy storage density (W_1) of the ceramics at different sintering temperatures is similar to the trend of the energy storage efficiency (η), as shown in Fig. 11(b). Both W_1 and η increase almost linearly with the increment in sintering temperatures and reach maximum values of 0.33 J/cm^3 and 41.7%, respectively at 1100°C, and then decrease. On the other hand, as the sintering temperatures increased from 1000°C to 1200°C, the values of W_2 of the samples increased from 0.37 to 0.55 J/cm^3, reaching the highest value of 0.55 J/cm^3 at 1050°C, following which it decreased.

From the experimental results above, we obtained the improvement of dielectric, ferroelectric and energy storage

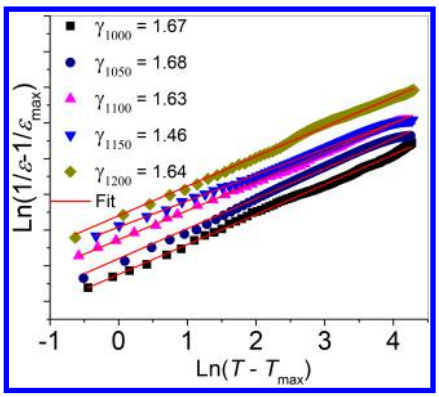

Fig. 9. Plotting $\ln(1/\varepsilon - 1/\varepsilon_{max})$ versus $\ln(T - T_m)$.

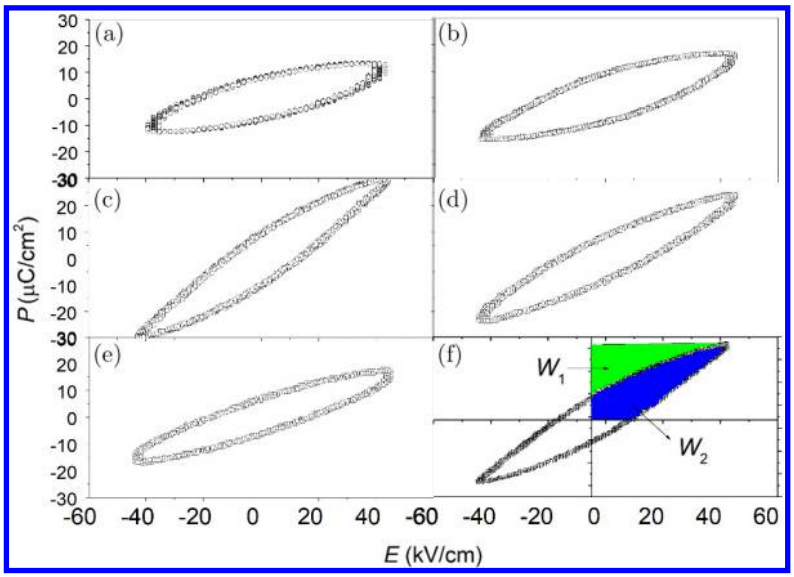

Fig. 10. $P-E$ hysteresis loops of the ceramics as a function of sintering temperature.

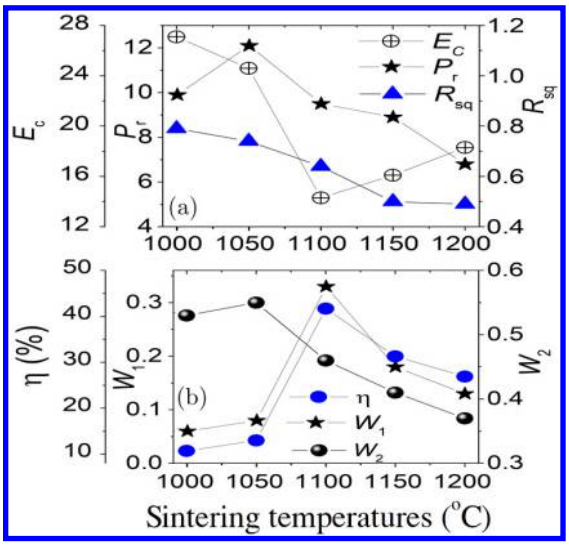

Fig. 11. The calculated the ferroelectric parameters of ceramics.

properties of lead-free $Bi_{0.5}(Na_{0.8}K_{0.2})_{0.5}(Ti_{0.96}Sn_{0.04})O_3$ ceramics for their various applications, including the dielectric and energy storage properties by optimizing the sintering temperature at 1100°C. As a result, the data of the characteristic parameters of the sample sintered at 1100°C, namely, the sintering temperature (T_s), Curie temperature (T_m), the dielectric constant (ε_{max}), the remnant polarization (P_r), coercive field (E_c), the energy storage density (W_1) and the energy storage efficiency (η) were extracted and compared with those of other Bi-based lead-free ceramics as listed in Table 3.[50–52] This study indicated that the $Bi_{0.5}(Na_{0.8}K_{0.2})_{0.5}(Ti_{0.96}Sn_{0.04})O_3$ ceramics can be obtained at a lower sintering temperature, while the electrical properties of the material ceramics are well-maintained.

4. Conclusions

The effects of sintering temperature on the structural, morphological the dielectric, ferroelectric and energy storage properties of $Bi_{0.5}(Na_{0.8}K_{0.2})_{0.5}(Ti_{0.96}Sn_{0.04})O_3$ lead-free ceramics were investigated. Experimental results showed that at the sintering temperature of 1100°C, the BNKTS ceramics exhibited excellent physical, dielectric, and ferroelectric properties: high density of 5.88 g. cm^{-3} (relative density 96.7% of the theoretical value); dielectric constant (ε_r) of 1215; low dielectric loss (tanδ) of 0.051; highest dielectric constant (ε_{max}) of 4335; high remanent polarization (P_r) of

Table 3. Compilation of physical properties for ceramics with other reported data.

Ceramics	T_S (°C)	T_m (°C)	ε_{max}	E_C (kv/cm)	P_r μC/cm^2	W_1 J/cm^3	η (%)	Ref.
$0.97Bi_{0.5}(Na_{0.8}K_{0.2})_{0.5}TiO_3$-$0.03(Ba_{0.70}Sr_{0.30})O_3$	1100	320	4318	20.7	12.7	—	—	50
$0.97Bi_{0.5}(Na_{0.8}K_{0.2})_{0.5}TiO_3$-$0.03(Ba_{0.70}Sr_{0.30})O_3$	1125	320	4982	17.85	16.7	—	—	50
$Bi_{0.5}(Na_{0.84}K_{0.16})_{0.5}TiO_3$	1125	300	4930	42.4	29.3	0.09	9	51
$0.97Bi_{0.5}(Na_{0.84}K_{0.16})_{0.5}TiO_3$-$0.03Ba(Nb_{0.01}Ti_{0.99})O_3$	1125	306	5350	16.7	23	0.28	20	51
$Bi_{0.5}(Na_{0.5}K_{0.5})_{0.5}TiO_3$	1150	300	3500	18.0	23.0	0.1	10	52
$0.98Bi_{0.5}(Na_{0.5}K_{0.5})_{0.5}TiO_3$-$0.02Ba_{0.9}Ca_{0.1}Ti_{0.9}Zr_{0.1}O_3$	1150	300	3500	18.0	23.0	0.37	50	52
$Bi_{0,5}(Na_{0.8}K_{0.2})_{0,5}(Ti_{0.96}Sn_{0.04})O_3$	1100	262	4335	14.3	9.5	0.33	41.7	This work

9.5 μC cm^{-2}; and high coercive field (E_c) of 14.3 kV/cm. Furthermore, the BNKTS ceramics are good candidates for lead-free applications with energy storage density up to 0.55 J/cm^3 and an efficiency of 41.7%.

Acknowledgment

This research was funded by Ministry of Education and Training under Grant No. B2019-DHH-13.

References

[1]W. Pan, M. Cao, J. Qi, H. Hao, Z. Yao, Z. Yu and H. Liu, Defect structure and dielectric behavior in $SrTi_{1-x}(Zn_{1/3}Nb_{2/3})_xO_3$ ceramics, *J. Alloy. Compd.* **784**(5), 1303 (2019).

[2]P. Fan, Y. Zhang, Q. Zhang, B. Xie, Y. Zhu, M. A. Mawat, W. Ma, K. Liu, J. Xiao and H. Zhang, Large strain with low hysteresis in $Bi_4Ti_3O_{12}$ modified $Bi_{1/2}(Na_{0.82}K_{0.18})_{1/2}TiO_3$ lead-free piezoceramics, *J. Eur. Ceram. Soc* **. 38**(13), 4404 (2018).

[3]P. D. Gio, H. Q. Viet and L. D. Vuong, Low-temperature sintering of $0.96(K_{0.5}Na_{0.5})NbO_3$-$0.04LiNbO_3$ lead-free piezoelectric ceramics modified with CuO, *Int. J. Mater. Res.* **109**(11), 1071 (2018).

[4]P. Li, J. Zhai, B. Shen, S. Zhang, X. Li, F. Zhu and X. Zhang, Ultrahigh piezoelectric properties in textured (K,Na)NbO_3-based lead-free ceramics, *Adv. Mater.* **30**(8), 1705171 (2018).

[5]K. Shibata, R. Wang, T. Tou and J. Koruza, Applications of lead-free piezoelectric materials, *MRS Bullet.* **43**(8), 612 (2018).

[6]L. D. Vuong and P. D. Gio, Enhancement in dielectric, ferroelectric, and piezoelectric properties of $BaTiO_3$- modified $Bi_{0.5}(Na_{0.4}K_{0.1})TiO_3$ lead-free ceramics, *J. Alloy. Compd.* **817**, 152790 (2020).

[7]D. V. Le and A. Q. Dao, Enhanced physical properties of $Bi_4Ti_3O_{12}$ modified $Bi_{0.5}(Na_{0.4}K_{0.1})TiO_3$ lead-free piezoelectric ceramics using crystallographic orientation techniques, *J. Electroceram.* **E** (2020).

[8]N. T. Tho, A. Inoue, M. Noda and M. Okuyama, Low temperature preparation of bismuth-related ferroelectrics powder and thin films by hydrothermal synthesis, *IEEE Trans. Ultrasonic. Ferroelec. Freq. Control* **54**, 2603 (2007).

[9]N. Truong-Tho and N. T. Nghi-Nhan, Fabrication by annealing at approximately 1030°C and electrical characterization of lead-free $(1-x)Bi_{0.5}K_{0.5}TiO_{3-x}Ba(Fe_{0.5}Nb_{0.5})_{0.05}Ti_{0.95}O_3$ piezoelectric ceramics, *J. Electron. Mater.* **46**(6), 3585 (2017).

[10]I. Coondoo, N. Panwar and A. Kholkin, Lead-free piezoelectrics: Current status and perspectives, *J. Adv. Dielectric.* **3**(2), 1330002 (2013).

[11]Y. R. Zhang, J. F. Li and B. P. Zhang, Enhancing electrical properties in NBT–KBT lead-free piezoelectric ceramics by optimizing sintering temperature, *J. Am. Ceram. Soc.* **91**(8), 2716 (2008).

[12]A. Sasaki, T. Chiba, Y. Mamiya and E. Otsuki, Dielectric and piezoelectric properties of $(Bi_{0.5}Na_{0.5})TiO_3$–$(Bi_{0.5}K_{0.5})TiO_3$ systems, *Jpn. J. Appl. Phys.* **38**, 5564 (1999).

[13]A. Inoue, T. T. Nguyen, M. Noda and M. Okuyama, Low temperature preparation of bismuth-related ferroelectrics by hydrothermal synthesis, *Proc. 2007 16th IEEE Int. Symp. Appl. Ferro*. **136**, 136 (2007).

[14]T. T. Nguyen, T. Kanashima and M. Okuyama, Leakage current reduction and ferroelectric property of $BiFe_{1-x}Co_xO_3$ thin films prepared by chemical solution deposition using rapid thermal annealing, *MRS Online Proc.* **1199**, 1199-F06-19 (2011).

[15]N. T. Tho, T. Kanashima, M. Sohgawa, D. Ricinschi, M. Noda and M. Okuyama, Ferroelectric properties of $Bi_{1.1}Fe_{1-x}Co_xO_3$ thin films prepared by chemical solution deposition using iterative rapid thermal annealing in N_2 and O_2, *Jpn. J. Appl. Phys.* **49**, 09MB05 (2010).

[16]N. T. Tho, T. Kanashima and M. Okuyama, Leakage current reduction and ferroelectric property of $BiFe_{1-x}Co_xO_3$ thin films prepared by chemical solution deposition using iterative rapid thermal Annealing at Approximately 520°C, *Jpn. J. Appl. Phys.* **49**, 095803 (2010).

[17]L. D. Vuong and N. T. Tho, The intering behavior and physical properties of Li_2CO_3-doped $Bi_{0.5}(Na_{0.8}K_{0.2})_{0.5}TiO_3$ lead-free ceramics, *Int. J. Mater. Res.* **108**, 1 (2017).

[18]L. D. Vuong and N. Truong-Tho, Effect of ZnO nanoparticles on the sintering behavior and physical properties of $Bi_{0.5}(Na_{0.8}K_{0.2})_{0.5}TiO_3$ lead-free ceramics, *J. Electro. Mater.* **46**(11), 6395 (2017).

[19]O. Mokhtari and H. Nishikawa, Transient liquid phase bonding of Sn–Bi solder with added Cu particles, *J. Mater. Sci. Mater. Electron.* **27**, 4232 (2016).

[20]L. Zhang, Z. Wang, Y. Li, P. Chen, J. Cai, Y. Yan, Y. Zhou, D. Wang and G. Liu, Enhanced energy storage performance in Sn doped $Sr_{0.6}(Na_{0.5}Bi_{0.5})_{0.4}TiO_3$ lead-free relaxor ferroelectric ceramics, *J. Eur. Ceram. Soc.* **39**(10), 3057 (2019).

[21]J. Xie, H. Hao, H. Liu, Z. Yao, Z. Song, L. Zhang, Q. Xu, J. Dai and M. Cao, Dielectric relaxation behavior and energy storage properties of Sn modified $SrTiO_3$ based ceramics, *Ceram. Int.* **42**(11), 12796 (2016).

[22]H. S. Han, W. Jo, J. K. Kang, C. W. Ahn, I. W. Kim, K. K. Ahn and J. S. Lee, Incipient Piezoelectrics and Electrostriction Behavior in Sn-doped $Bi_{1/2}(Na_{0.82}K_{0.18})_{1/2}TiO_3$ Lead-free Ceramics, *J. Appl. Phys.* **113**, 154102 (2013).

[23]J. S. Lee, K. N. Pham, H. S. Han, H. B. Lee and V. D. N. Tran, Strain enhancement of lead-free $Bi_{1/2}(Na_{0.82}K_{0.18})_{1/2}TiO_3$ ceramics by Sn doping, *J. Kor. Phys. Soc.* **60**(2), 212 (2012).

[24]A. Ullah, C. W. Ahn, A. Hussain and I. W. Kim, The effects of sintering temperatures on dielectric, ferroelectric and electric field-induced strain of lead-free $Bi_{0.5}(Na_{0.78}K_{0.22})_{0.5}TiO_3$ piezoelectric ceramics synthesized by the sol–gel technique, *Curr. Appl. Phys.* **10**(6), 1367 (2010).

[25]A. Hussain, C. W. Ahn, A. Ullah, J. S. Lee and I. W. Kim, The effect of sintering temperature on lead-free $Bi_{0.5}(Na_{0.78}K_{0.22})_{0.5}TiO_3$-$(Na_{0.5}K_{0.5})NbO_3$ ceramics, *Ferroelectric*, **404**(1) 157 (2010).

[26]T. Wang, X. Chen and Y. Qiu, Microstructure, depolarization temperature, and piezoelectric properties of $(Bi_{0.5}Na_{0.4}K_{0.1})Ti_{0.98}M_{0.02}O_{3-\delta}$ ($M^{3+} = Al^{3+}, Fe^{3+}$) lead-free ceramics, *Ferroelectric,* **510**(1), 161 (2017).

[27]M. S. Alkathy, A. Hezam, K. Manoja, J. Wang, C. Cheng, K. Byrappa and K. J. Raju, Effect of sintering temperature on structural, electrical, and ferroelectric properties of lanthanum and sodium co-substituted barium titanate ceramics, *J. Alloy. Compd.* **762**, 49 (2018).

[28]H. Naceur, A. Megriche and M. E. Maaoui, Effect of sintering temperature on microstructure and electrical properties of

$Sr_{1-x}(Na_{0.5}Bi_{0.5})_xBi_2Nb_2O_9$ solid solutions, *J. Adv. Ceram.* **3**(1), 17 (2014).
[29]N. D. Quan, V. N. Hung and D. D. Dung, Effect of Zr doping on structural and ferroelectric properties of lead-free $Bi_{0.5}(Na_{0.80}K_{0.20})_{0.5}TiO_3$ films, *J. Electro. Mater.* **46**, 5814 (2017).
[30]A. L. Hector and S. B. Wiggin, Synthesis and structural study of stoichiometric $Bi_2Ti_2O_7$ pyrochlore, *J. Solid Stat. Chem.* **177**(1), 139 (2004).
[31]Y. F. Kargin, S. Ivicheva and V. Volkov, Phase relations in the Bi_2O_3-TiO_2 system, *Rus. J. Inorganic Chem.* **60**(5), 619 (2015).
[32]D. D. Dung, N. V. Quyet and L. H. Bac, Role of sintering temperature on giant field-induced strain in lead-free $Bi_{0.5}(Na,K)_{0.5}TiO_3$-based ceramics, *Ferroelectric,* **474**(1), 113 (2015).
[33]N. D. T. Luan, L. D. Vuong, T. V. Chuong and N. T. Tho, Structure and physical properties of PZT-PMnN-PSN ceramics near the morphological phase boundary, *Adv. Mater. Sci. Eng.* **2014.E**, 1 (2014).
[34]R. M. German, *Liquid Phase Sintering* (Springer Science & Business Media, New York, 2013).
[35]C. Y. Luo, M. Z. Hu, Q. Huang, Y. Fu and H. S. Gu, Influence of ZnO and Nb_2O_5 additions on sintering behavior and microwave dielectric properties of $(Mg_{0.95}Ca_{0.05})$ TiO_3 ceramics, *Key Eng. Mater.* **512**, 1184 (2012).
[36]J. Hao, B. Shen, J. Zhai and H. Chen, Effect of BiMeO3 on the phase structure, ferroelectric stability, and properties of lead-free Bi0.5(Na0.80K0.20)0.5TiO3 ceramics, *J. Am. Ceram. Soc.* **97**(6), 1776 (2014).
[37]H. Luo, H. Ke, H. Zhang, L. Zhang, F. Li, L. Cao, P. Guo, D. Jia and Y. Zhou, Bi-fluctuation in $Na_{0.5}Bi_{0.5}TiO_3$ ferroelectric ceramics with abnormal relaxor behaviour, *Philos. Mag.* **99**(21), 2661 (2019).
[38]Y. Zhao, X. Liu, J. Shi, J. He, H. Du and H. Lu, Enhanced high temperature stability of BNT-BKT-CBTZ lead-free dielectrics, *ECS J. Solid. State. Sci. Technol.* **8**(12) (2019) N201.
[39]A. Maqbool, A. Hussain, R. A. Malik, J. U. Rahman, A. Zaman, T. K. Song, W. J. Kim and M. H. Kim, Evolution of phase structure and giant strain at low driving fields in Bi-based lead-free incipient piezoelectrics, *Mater. Sci. Eng. B*, **199**, 105 (2015).
[40]C. Xu, D. Lin and K. Kwok, Structure, electrical properties and depolarization temperature of $(Bi_{0.5}Na_{0.5})TiO_3$–$BaTiO_3$ lead-free piezoelectric ceramics, *Solid State Sci.* **10**(7), 934 (2008).
[41]Y. Sung, J. Kim, J. Cho, T. Song, M. Kim, H. Chong, T. Park, D. Do and S. Kim, Effects of Na nonstoichiometry in $(Bi_{0.5}Na_{0.5+x})TiO_3(Bi_{0.5}Na_{0.5+x})TiO_3$ ceramics, *Appl. Phys. Lett.* **96**(2), 022901 (2010).
[42]P. Butnoi, S. Manotham, P. Jaita, K. Pengpat, S. Eitssayeam, T. Tunkasiri and G. Rujijanagul, Effects of processing parameter on phase transition and electrical properties of lead-free BNKT piezoelectric ceramics, *Ferroelectrics.* **511**(1), 42 (2017).
[43]K. Yoshii, Y. Hiruma, H. Nagata and T. Takenaka, Electrical properties and depolarization temperature of $(Bi_{1/2}Na_{1/2})TiO_3$–$(Bi_{1/2}K_{1/2})TiO_3$ lead-free piezoelectric ceramic, *Jpn. J. Appl. Phys.* **45**(5S), 4493 (2006).
[44]L. M. Chang, Y. D. Hou, M. K. Zhu and H. Yan, Effect of sintering temperature on the phase transition and dielectrical response in the relaxor-ferroelectric-system 0.5PZN–0.5PZT, *J. Appl. Phys.* **101**(3), 034101 (2007).
[45]J. U. Rahman, A. Hussain, A. Maqbool, R. A. Malik, M. S. Kim and M. H. Kim, Effect of sintering temperature on the electromechanical properties of $0.945Bi_{0.5}Na_{0.5}TiO_3$-$0.055BaZrO_3$ ceramics, *J. Kor. Phys. Soc.* **66**(7), 1072 (2015).
[46]N. Dong, X. Gao, F. Xia, H. Liu, H. Hao and S. Zhang, Dielectric and piezoelectric properties of textured lead-free $Na_{0.5}Bi_{0.5}TiO_3$-based ceramics, *Cryst.* **9**(4), 206 (2019).
[47]R. Sumang, W. Buasri, N. Kumar and T. Bongkarn, Influence of sintering temperature on crystal structure, microstructure and electrical properties of BNT-BKT-BZT piezoelectric ceramic, *Integrat. Ferroelectr.* **187**(1), 181 (2018).
[48]R. Cao, G. Li, J. Zeng, S. Zhao, L. Zheng and Q. Yin, The piezoelectric and dielectric properties of $0.3Pb(Ni_{1/3}Nb_{2/3})O_3$–$x$ $PbTiO_3$–$(0.7-x)PbZrO_3$ ferroelectric ceramics near the morphotropic phase boundary, *J. Ame. Ceram. Soc.* **93**(3), 737 (2010).
[49]X. Liu, J. Shi, F. Zhu, H. Du, T. Li, X. Liu and H. Lu, Ultrahigh energy density and improved discharged efficiency in bismuth sodium titanate based relaxor ferroelectrics with A-site vacancy, *J. Materiom.* **4**(3), 202 (2018).
[50]P. Jaita, S. Manotham and N. Lertcumfu, Influence of sintering temperature on structure and electrical properties of modified-BNKT lead-free piezoelectric ceramics, *Trans. Tech. Publ.* **777**, 55 (2018).
[51]S. Manotham, P. Butnoi, P. Jaita, N. Kumar, K. Chokethawai, G. Rujijanagul and D. P. Cann, Large electric field-induced strain and large improvement in energy density of bismuth sodium potassium titanate-based piezoelectric ceramics, *J. Alloy. Compd.* **739**, 457 (2018).
[52]D. K. Kushvaha, S. K. Rout and B. Tiwari, Structural, piezoelectric and highdensity energy storage properties of lead-free BNKT-BCZT solid solution, *J. Alloy. Compd.* **782**, 270 (2018).